Copy
RM L53H14a

NACA

RESEARCH MEMORANDUM

LOW-SPEED LONGITUDINAL CHARACTERISTICS OF TWO UNSWEPT WINGS OF HEXAGONAL AIRFOIL SECTIONS HAVING ASPECT RATIOS OF 2.5 AND 4.0 WITH FUSELAGE AND WITH HORIZONTAL TAIL LOCATED AT VARIOUS VERTICAL POSITIONS

By William M. Hadaway and Patrick A. Cancro

Langley Aeronautical Laboratory
Langley Field, Va.

NATIONAL ADVISORY COMMITTEE
FOR AERONAUTICS

WASHINGTON

October 26, 1953

NATIONAL ADVISORY COMMITTEE FOR AERONAUTICS

RESEARCH MEMORANDUM

LOW-SPEED LONGITUDINAL CHARACTERISTICS OF TWO UNSWEPT WINGS OF HEXAGONAL AIRFOIL SECTIONS HAVING ASPECT RATIOS OF 2.5 AND 4.0 WITH FUSELAGE AND WITH HORIZONTAL TAIL LOCATED AT VARIOUS VERTICAL POSITIONS

By William M. Hadaway and Patrick A. Cancro

SUMMARY

Investigations have been made in the Langley 19-foot pressure tunnel to determine the low-speed horizontal-tail effectiveness and static longitudinal characteristics of two model configurations having unswept wings with aspect ratios of 4.0 and 2.5. Each wing had a taper ratio of 0.625 and hexagonal airfoil sections with 6-percent-thick chords. The wings were mounted on circular fuselages and tests were made with and without full-span drooped leading edges and part-span inboard trailing-edge flaps. Three horizontal tail positions, two above and one below the wing-chord plane, were investigated. Tests of both wings were made at a Mach number of 0.15 corresponding to Reynolds numbers of 6.2×10^6 for the aspect-ratio-4.0 wing and 7.6×10^6 for the aspect-ratio-2.5 wing. The data of the aspect-ratio-2.5 wing presented herein for comparison with the aspect-ratio-4.0 wing are part of a more extensive investigation reported in NACA RM L52L11b.

Results indicate that the horizontal tails of plain-wing configurations having aspect ratios of 2.5 and 4.0 were exerting a stabilizing influence at all angles of attack and at all vertical-tail positions tested, except just below maximum lift with the tail located 17.7-percent semispan above the fuselage on the aspect-ratio-2.5 wing configuration, in which case the tail was destabilizing.

With flaps deflected, the tails were stabilizing for all vertical positions and at all angles of attack, except near 0° for the aspect-ratio-2.5 wing configuration with the tail 17.7-percent semispan below

the fuselage and beyond maximum lift on the aspect-ratio-4.0 wing configuration with the tail 17.7-percent semispan above the fuselage.

In most instances, the tail effectiveness of the aspect-ratio-4.0 wing configuration was better than that of the aspect-ratio-2.5 wing for corresponding tail positions and flap configurations.

INTRODUCTION

As part of a general investigation of thin unswept low-aspect-ratio wings by the National Advisory Committee for Aeronautics, tests of a model having a wing of aspect ratio 4.0 have been conducted in the Langley 19-foot pressure tunnel in order to evaluate the low-speed horizontal tail effectiveness and longitudinal characteristics and to compare the characteristics of this model with those of a similar model having a wing of aspect ratio 2.5. Both wings had hexagonal airfoil sections with 6-percent-thick chords. Test configurations included a combination of leading- and trailing-edge flaps both deflected and undeflected on the wing-body combination with and without a horizontal tail. The ratios of tail spans, tail lengths, and tail heights to the wing span were held constant on the two models for comparison purposes. It should be pointed out that results presented in this paper for the aspect-ratio-2.5 wing were reported previously in reference 1.

Aileron investigations of the two wings are presented in references 2 and 3.

Tests of the aspect-ratio-4.0 configuration were made at a Reynolds number of 6.2×10^6 and those of the aspect-ratio-2.5 configuration were made at a Reynolds number of 7.6×10^6.

SYMBOLS

The data are referred to wind axes with the origin at the 0.25 mean aerodynamic chord projected to the plane of symmetry. Symbols and coefficients are defined as follows:

C_L lift coefficient, Lift/qS

C_D drag coefficient, Drag/qS

C_m pitching-moment coefficient, Pitching moment/qS$\bar{c}$

α	angle of attack, deg
S	wing area, sq ft
$\bar{c}$	wing mean aerodynamic chord, $\frac{2}{S}\int_0^{b/2} c^2 dy$, ft
b	wing span, ft
z	vertical position of horizontal tail from wing-chord plane (positive up), ft
q	dynamic pressure, $\rho V^2/2$
c	local wing chord, ft
y	spanwise ordinate, ft
ρ	density of air, slugs/cu ft
V	wind velocity, ft/sec
R	Reynolds number, $\rho V\bar{c}/\mu$
A	aspect ratio
μ	viscosity of air, slugs/ft-sec
τ	horizontal tail-effectiveness parameter
$\left(C_{L_\alpha}\right)_t$	tail lift-curve slope
$\left(q_t/q\right)_e$	ratio of effective dynamic pressure at tail to free-stream dynamic pressure
ϵ_e	effective downwash angle, deg
$C_{m_{i_t}}$	rate of change of pitching-moment coefficient with horizontal-tail incidence angle
$C_{m_{i_{t_0}}}$	rate of change of pitching-moment coefficient with horizontal-tail incidence angle for any tail position and flap configuration at 0° angle of attack

$\left(C_{m_{i_t}}\right)_0'$ value of $C_{m_{i_t}}$ at 0° for high tail position with flaps off (assumed interference-free conditon)

$dC_{m_t}/d\alpha$ rate of change of pitching-moment coefficient due to tail with angle of attack

η tail efficiency factor, $\left(C_{m_{i_t}}\right)_0 \Big/ \left(C_{m_{i_t}}\right)_0'$

i_t angle of incidence of horizontal tail measured with respect to wing-chord plane, positive when trailing edge moves down, deg

l horizontal-tail length, distance in wing-chord plane from quarter-chord point of wing mean aerodynamic chord to quarter-chord point of horizontal-tail mean aerodynamic chord, ft

δ_f angle of deflection of plain trailing-edge flaps, deg

δ_n angle of deflection of drooped-nose flaps, deg

$d\epsilon/d\alpha$ rate of change of effective downwash angle with angle of attack

$\bar{V}$ tail volume, $\frac{S_t}{S}\frac{l}{\bar{c}}$

Λ angle of sweep

Subscripts and abbreviations:

t horizontal tail

0 value at 0° angle of attack (flaps neutral)

e effective

w wing

MODEL

Details of the wings, fuselages, and horizontal tails are shown in figure 1. Both wings were constructed of solid steel and had taper ratios of 0.625, symmetrical hexagonal airfoil sections of 6-percent-thickness chord that were parallel to the plane of symmetry, and 0° sweep of the 50-percent-chord line. The leading- and trailing-edge angles were 11.42° and the upper and lower surfaces of each airfoil surface were parallel between 0.30c and 0.70c for both wings. The aspect-ratio-4.0 wing tips were round and had an elliptical cross section and the aspect-ratio-2.5 wing tips had a wedge-shaped cross section. The leading edge of each wing could be drooped at the 0.15-chord line from the wing-fuselage juncture to spanwise station $0.95b/2$. Likewise, the trailing edge of each wing could be deflected about the 0.75-chord line from the wing-fuselage juncture to station $0.95b/2$. Each trailing-edge flap was divided at the $0.55b/2$ spanwise station on both the aspect-ratio-4.0 wing and the aspect-ratio-2.5 wing.

Both wings were tested with and without a cylindrical mahogany fuselage mounted at the midfuselage position at 0° incidence. The fineness ratio was 10:1 for the fuselage of the aspect-ratio-4.0 wing and 8:1 for the fuselage of the aspect-ratio-2.5 wing. The fuselages were attached to the two wings in such a manner that the ratio $\frac{l}{b_w/2}$ of 1.660 for the aspect-ratio-4.0 wing was approximately equal to that of the aspect-ratio-2.5 wing (1.628). Also, the spans of the tails were such that the values of the ratio b_t/b_w of 0.499 were equal for the two configurations. The horizontal tail of both configurations employed NACA 0012 airfoil sections with 0° sweep of the 50-percent-chord line. The tail of the aspect-ratio-4.0 wing had an aspect ratio of 4.18, a taper ratio of 0.525, and a ratio of tail area to wing area of 0.238; whereas the tail of the aspect-ratio-2.5 wing had an aspect ratio of 3.12, a taper ratio of 0.625, and a ratio of tail area to wing area of 0.20. The tail was attached to the fuselage by means of a strut and could be located vertically at either $0.40b_w/2$ or $0.177b_w/2$ above or $0.177b_w/2$ below the wing-chord plane extended for both the aspect-ratio-4.0 and aspect-ratio-2.5 configurations. The incidence of either tail measured with respect to the wing-chord plane could be varied through an angle range from 6° to -6° in increments of 2°.

A two-support system was used in testing the plain wings and a three-support system (shown in fig. 2) was employed for all tests with a fuselage.

TESTS

Tests were conducted in the Langley 19-foot pressure tunnel with the tunnel air compressed to 33 lb/sq in. abs. For the aspect-ratio-4.0 wing configuration, all tests were conducted at a Reynolds number of 6.2×10^6 and a corresponding Mach number of 0.15; tests of the aspect-ratio-2.5 configuration were made at a Reynolds number of 7.6×10^6 and a corresponding Mach number of 0.15. The configurations tested were the plain wings with and without a fuselage (fig. 3) and the wing-fuselage combinations with full-span leading-edge flaps deflected 30° and inboard part-span plain trailing-edge flaps deflected 50° (fig. 4). The flap-deflection angles used for comparison ($\delta_n = 30°$; $\delta_f = 50°$) are considered among the most favorable tested for a wing of similar plan form and airfoil section (ref. 4). The effects of a horizontal tail at various vertical stations were investigated for the wing-fuselage configuration of both wings with and without flaps deflected. Lift, drag, and pitching-moment measurements were obtained through an angle-of-attack range from -4° to 24°.

Lift characteristics of the two horizontal tails tested alone are presented in figure 5. The tail of the aspect-ratio-2.5 wing was tested at Reynolds numbers of 3.0×10^6 and 2.3×10^6, corresponding to values of 7.6×10^6 and 5.7×10^6 based on the wing $\bar{c}$ (ref. 1). The tail of the aspect-ratio-4.0 wing was tested at Reynolds numbers of 2.8×10^6 and 1.0×10^6, corresponding to values of 6.2×10^6 and 2.1×10^6 based on the wing $\bar{c}$. The lift-curve slope $C_{L_{\alpha_t}}$ of the tail used with the aspect-ratio-2.5 wing was constant to approximately 23° for both Reynolds numbers, and the value of $C_{L_{\alpha_t}}$ for the tail used with the aspect-ratio-4.0 wing was constant to approximately 16° for both values of Reynolds number tested.

Studies of the flow over the upper surface of the two wings were made at various angles of attack with and without leading- and trailing-edge flaps deflected by observing the action of wool tufts attached to the wing upper surfaces at various chordwise and spanwise positions. These tests were made with a fuselage attached, except for the aspect-ratio-2.5 wing configuration with flaps undeflected. Sketches based on these observations are presented in figure 6. Flow studies were also made by observing the action of a mixture of kerosene and lampblack in the stalled region of the aspect-ratio-4.0 wing-body combination with and without flaps deflected. The procedure employed was to allow the mixture of lampblack and kerosene to flow onto the wing through a tube

at the end of a strut-mounted probe. With this probe it was possible to release the mixture at any spanwise or chordwise position desired, as can be seen in figure 7.

CORRECTIONS TO DATA

The lift, drag, and pitching-moment coefficients have been corrected for support tare and interference effects, and the angle of attack has been corrected for airstream misalinement and jet-boundary effects. Jet-boundary corrections were also applied to the drag coefficients and pitching-moment coefficients with tail on, but were considered negligible for tail-off pitching-moment coefficients and were not applied. The jet-boundary corrections were calculated by the method of reference 5.

REDUCTION OF DATA

Effective Downwash and Dynamic Pressure

For both aspect-ratio-4.0 and aspect-ratio-2.5 wing configurations, the values of ϵ_e and $\left(q_t/q\right)_e$ were obtained from the pitching-moment data for three or more incidence angles at each tail height investigated. Since the isolated tail tests indicated $C_{L_{\alpha_t}}$ to be constant to high values of α_t, the methods of determining ϵ_e and $\left(q_t/q\right)_e$ were simplified to

$$\epsilon_e = \alpha + i_t - \alpha_t$$

where

$$\alpha_t = \frac{C_{m_t}}{C_{m_{i_t}}}$$

The values of effective dynamic-pressure ratio $\left(q_t/q\right)_e$ at the tail were determined by computing the ratio of the values of $C_{m_{i_t}}$ obtained

through the angle-of-attack ranges of the various configurations to the values of $C_{m_{i_t}}$ for the comparable tail height of the flap-neutral configuration at zero lift.

Tail Efficiency Factor

The lift-curve slope of the horizontal tail may be altered because of the interference effects of the wing-fuselage combination, and a tail effeciency factor η has been used to represent the effective change in $C_{L_{\alpha_t}}$. The values of η were calculated on the assumption that the tail located at $z = 0.400b/2$ was 100 percent efficient since the distance from the fuselage was large and the interference effects of the tail support were considered to be small. The values of η were obtained from the relation $C_{m_{i_{t_0}}} \Big/ \left(C_{m_{i_t}}\right)'_0$ for each tail position and configuration. The following table presents values of $C_{m_{i_{t_0}}}$ and η calculated for configurations with flaps in a neutral position:

Tail height	Aspect-ratio-4.0 configurations		Aspect-ratio-2.5 configurations	
	$C_{m_{i_{t_0}}}$	η	$C_{m_{i_{t_0}}}$	η
0.400b/2	-0.0472	1.000	-0.0202	1.000
.177b/2	-.0442	.94	-.0189	.94
-.177b/2	-.0430	.91	-.0190	.94

Tail Effectiveness Parameter

A tail effectiveness parameter τ which combines the effects of both the dynamic-pressure variations and the downwash angle on the

stability contribution of the horizontal tail is derived in reference 6 and is defined as

$$\frac{dC_{m_t}}{d\alpha}\frac{1}{\left(C_{L_\alpha}\right)_t \bar{V}} = \tau = -\eta\left[\left(\frac{q_t}{q}\right)_e\left(1 - \frac{d\epsilon_e}{d\alpha}\right) + \alpha_t \frac{\partial\left(\frac{q_t}{q}\right)_e}{\partial\alpha}\right]$$

Negative values of τ indicate that the tail is contributing stability to the model configuration. Examination of the aforementioned equation indicates that, when the tail is out of the wake and $\partial\left(\frac{q_t}{q}\right)_e/\partial\alpha$ approaches zero, values of τ are independent of tail load and are, consequently, independent of trim condition and the center-of-gravity location of the model. For angles of attack where the tail enters the wake, however, finite values of $\partial\left(\frac{q_t}{q}\right)_e/\partial\alpha$ are obtained and the values of τ are dependent on the tail load. The values of τ presented herein are applicable to the model when trimmed with the center of gravity at $0.25\bar{c}$ and were calculated from the relationship

$$\tau = -\eta\left[\left(\frac{q_t}{q}\right)_e\left(1 - \frac{d\epsilon_e}{d\alpha}\right) + \alpha_t \frac{\partial\left(\frac{q_t}{q}\right)_e}{\partial\alpha}\right]$$

after α_t had been determined to provide trim at each angle of attack.

RESULTS

Comparisons of lift, drag, and pitching-moment coefficients of the aspect-ratio-4.0 wing with those of the aspect-ratio-2.5 wing are presented in figures 3 and 4. Data from tests of the isolated horizontal tail are presented in figure 5. Figure 6 shows stall patterns as determined by tuft studies of both wings and figure 7 shows results of lampblack and kerosene studies on the aspect-ratio-4.0 wing. The effects of a horizontal tail on C_m, ϵ_e, and $\left(q_t/q\right)_e$ are indicated for both wings with flaps neutral and deflected in figures 8 and 9, respectively, for various representative tail heights at nearly constant incidence angles. Figure 10 presents a summary plot comparison of the tail-effectiveness

values of the aspect-ratio-4.0 configurations with those of the aspect-ratio-2.5 configurations at various tail heights.

On both the aspect-ratio-4.0 and aspect-ratio-2.5 wings having flaps undeflected, the flow separated along the leading edges of the inboard sections at low angles of attack and reattached at about the 15-percent-chord line (fig. 6). With increase in angle of attack, the leading-edge separation spread toward the wing tips and then did not reattach as the angle approached that for maximum lift. Accompanying rearward shifts in center of pressure are indicated by the pitching-moment curves of figure 3. As the angle of attack was increased further, the separated flow region moved outboard until it engulfed the entire wing. The marked change in the area of separated flow on both plain-wing configurations at moderate angles of attack is characteristic of wings having unswept, sharp leading edges and low ratios of thickness to chord (ref. 7).

The addition of leading- and trailing-edge flaps delayed the onset of separation to larger angles of attack for both the aspect-ratio-2.5 and aspect-ratio-4.0 configurations and increased the maximum lift coefficient about 0.6 in both instances. The flaps also confined the initial stall along the entire chord of the wing to the inboard sections and the stall progression toward the wing tips was more gradual with increase in angle of attack than on the plain-wing configurations.

Figure 7 gives an indication of the direction of flow at the surface of the aspect-ratio-4.0 wing-fuselage combination in the region beyond maximum lift with flaps both undeflected and deflected.

Figure 10 indicates that the horizontal tail of the plain-wing aspect-ratio-4.0 configuration was contributing more stability than that of the aspect-ratio-2.5 configuration for all tail positions tested to maximum lift. The stabilizing effect of the high tail position $\left(\frac{z}{b/2} = 0.400\right)$ on the aspect-ratio-2.5 plain-wing configuration was small at angles of attack near maximum lift, and the tail located just above the fuselage $\left(\frac{z}{b/2} = 0.177\right)$ was destabilizing at angles just below maximum lift; otherwise, the tails of both plain-wing configurations were exerting a stabilizing influence at all tail positions and angles of attack tested.

When leading- and trailing-edge flaps were deflected, all horizontal-tail positions of the aspect-ratio-4.0 wing configuration were contributing more stability than the corresponding tail positions of the aspect-ratio-2.5 wing configuration for most angles of attack to maximum lift. The exceptions were at angles of attack near maximum lift with the tail just

above the fuselage $\left(\frac{z}{b/2} = 0.177\right)$, where the tail of the aspect-ratio-4.0 wing began to be destabilizing; and at angles of attack just below maximum lift with the tail below the fuselage $\left(\frac{z}{b/2} = -0.177\right)$, where the effectiveness values seemed to be about the same for both configurations. With flaps deflected, the tail of the aspect-ratio-2.5 wing configuration located just below the fuselage $\left(\frac{z}{b/2} = -0.177\right)$ was slightly destabilizing at angles near 0°. The tail effectiveness of the aspect-ratio-4.0 model was better than that of the aspect-ratio-2.5 model for most of the conditions tested, primarily because the values of $d\epsilon_e/d\alpha$ were, in general, smaller throughout the angle-of-attack range for the aspect-ratio-4.0 configurations (figs. 8(b) and 9(b)) as was expected. The variations of $(q_t/q)_e$ were generally in agreement for the two unflapped wings; however, with flaps deflected, the $(q_t/q)_e$ values of the aspect-ratio-4.0 wing were generally higher. Both lower values of $d\epsilon_e/d\alpha$ and higher values of $(q_t/q)_e$ tend to make the horizontal tail for the aspect-ratio-4.0 wing configuration more stabilizing.

CONCLUSIONS

A comparison was made of the low-speed longitudinal characteristics of two unswept wings of hexagonal airfoil sections having aspect ratios of 2.5 and 4.0 with fuselage and with horizontal tail located at various vertical positions. The following conclusions are presented:

1. The horizontal tails of the plain-wing configurations exerted a stabilizing influence at all angles of attack and at all vertical-tail positions tested, except just below maximum lift with the tail located 17.7-percent semispan above the fuselage on the aspect-ratio-2.5 wing configuration, in which case the tail was destabilizing.

2. With flaps deflected, the tails were stabilizing for all vertical positions and at all angles of attack except near 0° for the aspect-ratio-2.5 wing configuration with the tail 17.7-percent semispan below the fuselage and beyond maximum lift on the aspect-ratio-4.0 wing configuration with the tail 17.7-percent semispan above the fuselage.

3. In most instances, the tail effectiveness of the aspect-ratio-4.0 wing configuration was better than that of the aspect-ratio-2.5 wing for corresponding tail positions and flap configurations.

Langley Aeronautical Laboratory,
National Advisory Committee for Aeronautics,
Langley Field, Va., August 13, 1953.

REFERENCES

1. Foster, Gerald V., Mollenberg, Ernst F., and Woods, Robert L.: Low-Speed Longitudinal Characteristics of an Unswept Hexagonal Wing With and Without a Fuselage and a Horizontal Tail Located at Various Positions at Reynolds Numbers From 2.8×10^6 to 7.6×10^6. NACA RM L52L11b, 1953.

2. Fitzpatrick, James E., and Woods, Robert L.: Low-Speed Lateral-Control Characteristics of an Unswept Wing With Hexagonal Airfoil Sections and Aspect Ratio 2.5 Equipped With Spoilers and With Sharp- and Thickened-Trailing-Edge Flap-Type Ailerons at a Reynolds Number of 7.6×10^6. NACA RM L52B15, 1952.

3. Hadaway, William M.: Low-Speed Lateral Control Characteristics of an Unswept Wing With Hexagonal Airfoil Sections and Aspect Ratio 4.0 at a Reynolds Number of 6.2×10^6. NACA RM L53A29, 1953.

4. Johnson, Ben H., Jr., and Bandettini, Angelo: Investigation of a Thin Wing of Aspect Ratio 4 in the Ames 12-Foot Pressure Wind Tunnel. II - The Effect of Constant-Chord Leading- and Trailing-Edge Flaps on the Low-Speed Characteristics of the Wing. NACA RM A8F15, 1948.

5. Sivells, James C., and Salmi, Rachel M.: Jet-Boundary Corrections for Complete and Semispan Swept Wings in Closed Circular Wind Tunnels. NACA TN 2454, 1951.

6. Foster, Gerald V., and Griner, Roland F.: Low-Speed Longitudinal and Wake Air-Flow Characteristics at a Reynolds Number of 5.5×10^6 of a Circular-Arc 52° Sweptback Wing With a Fuselage and a Horizontal Tail at Various Vertical Positions. NACA RM L51C30, 1951.

7. Rose, Leonard M., and Altman, John M.: Low-Speed Investigation of the Stalling of a Thin, Faired, Double-Wedge Airfoil With Nose Flap. NACA TN 2172, 1950.

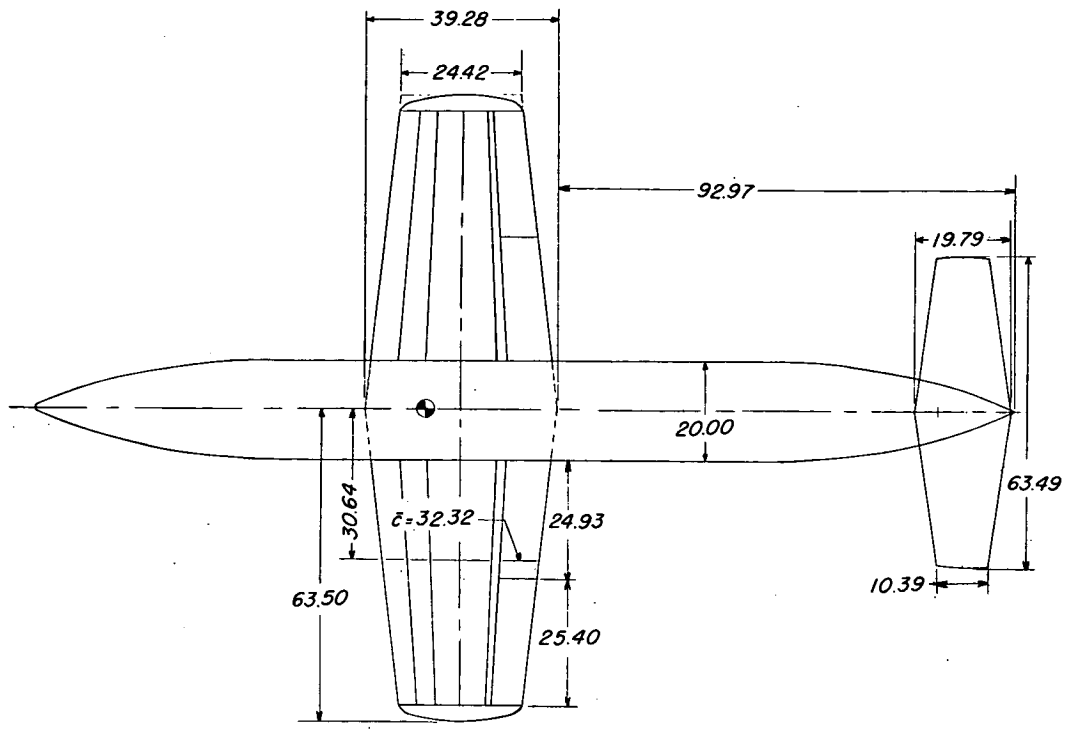

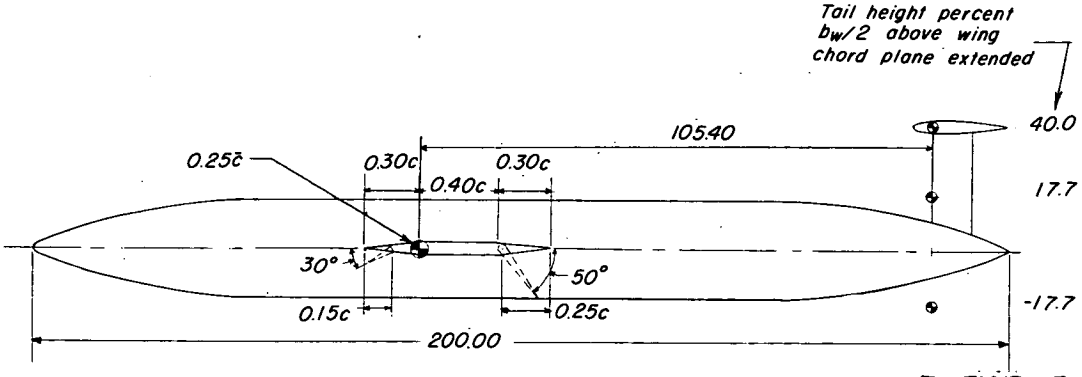

Double-wedge wing		Horizontal tail	
Aspect ratio	4.0	Airfoil section	NACA 0012
Area	4032.0 sq in.	Aspect ratio	4.18
Taper ratio	0.625	Area	961.5 sq in.
Thickness	0.06c	Taper ratio	0.525
Mean aerodynamic chord	32.32 in.	Span	63.49 in.
Span	127.00 in.	Mean aerodynamic chord	15.18 in.
$\Lambda_{c/4}$	3.36°		

(a) Aspect ratio, 4.0.

Figure 1.- Details of the wings, fuselages, and horizontal tails. All dimensions are in inches unless otherwise noted.

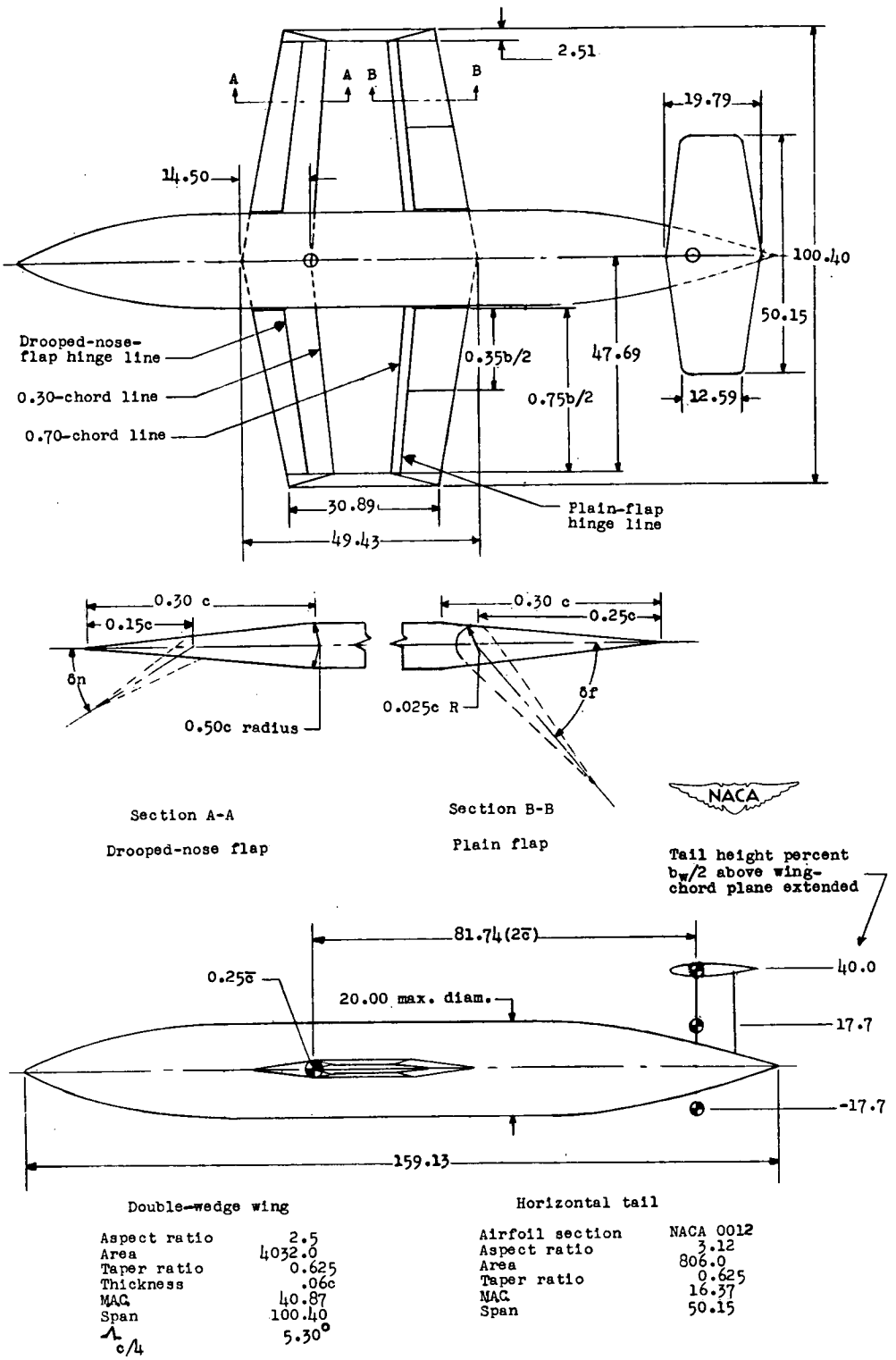

Double-wedge wing

Aspect ratio	2.5
Area	4032.0
Taper ratio	0.625
Thickness	.06c
MAC	40.87
Span	100.40
$\Lambda_{c/4}$	5.30°

Horizontal tail

Airfoil section	NACA 0012
Aspect ratio	3.12
Area	806.0
Taper ratio	0.625
MAC	16.37
Span	50.15

(b) Aspect ratio, 2.5.

Figure 1.- Concluded.

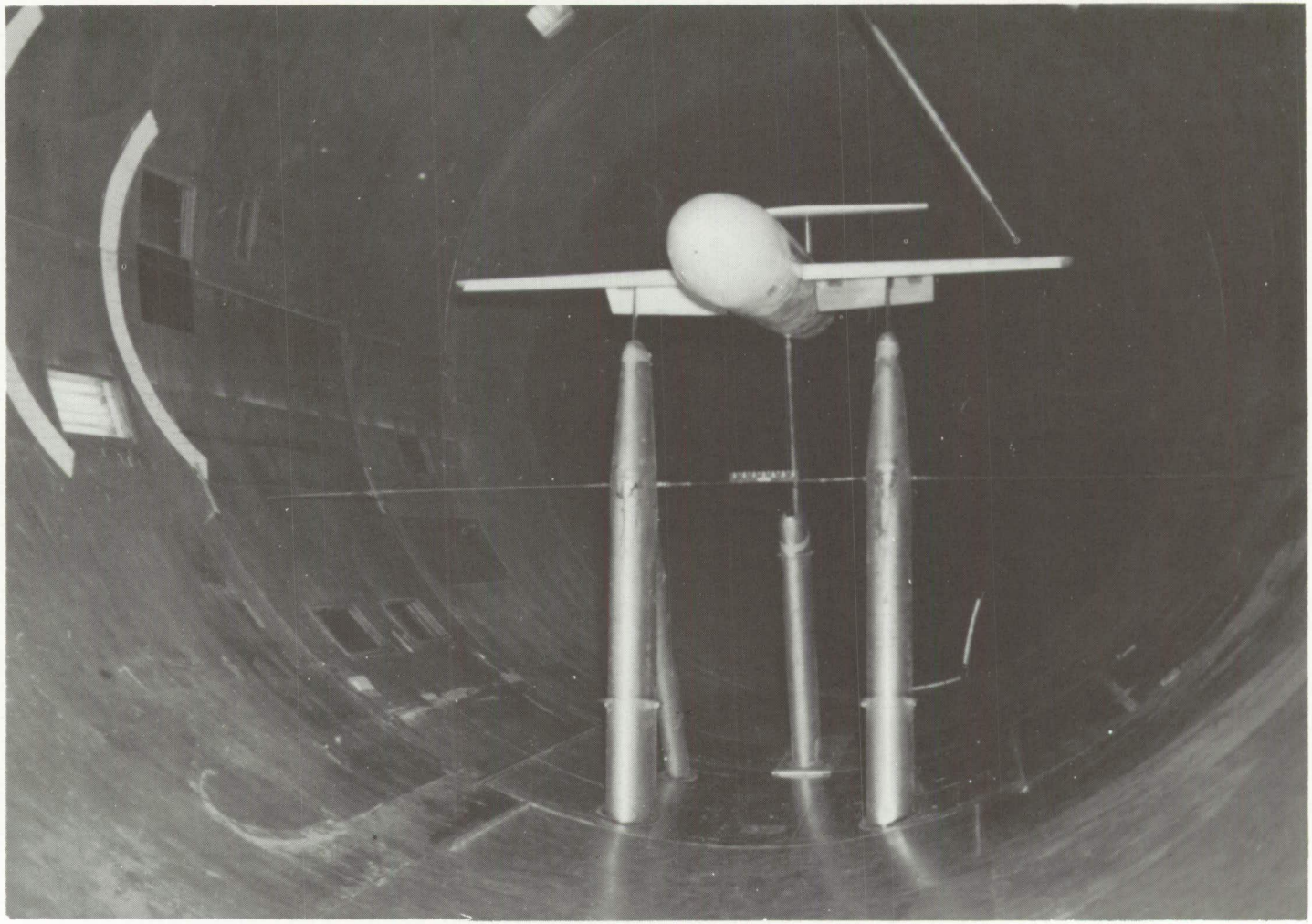

L-75706

Figure 2.- Front view of wing-fuselage horizontal-tail configuration with leading- and trailing-edge flaps deflected. Three-support system installation. Aspect ratio, 4.0.

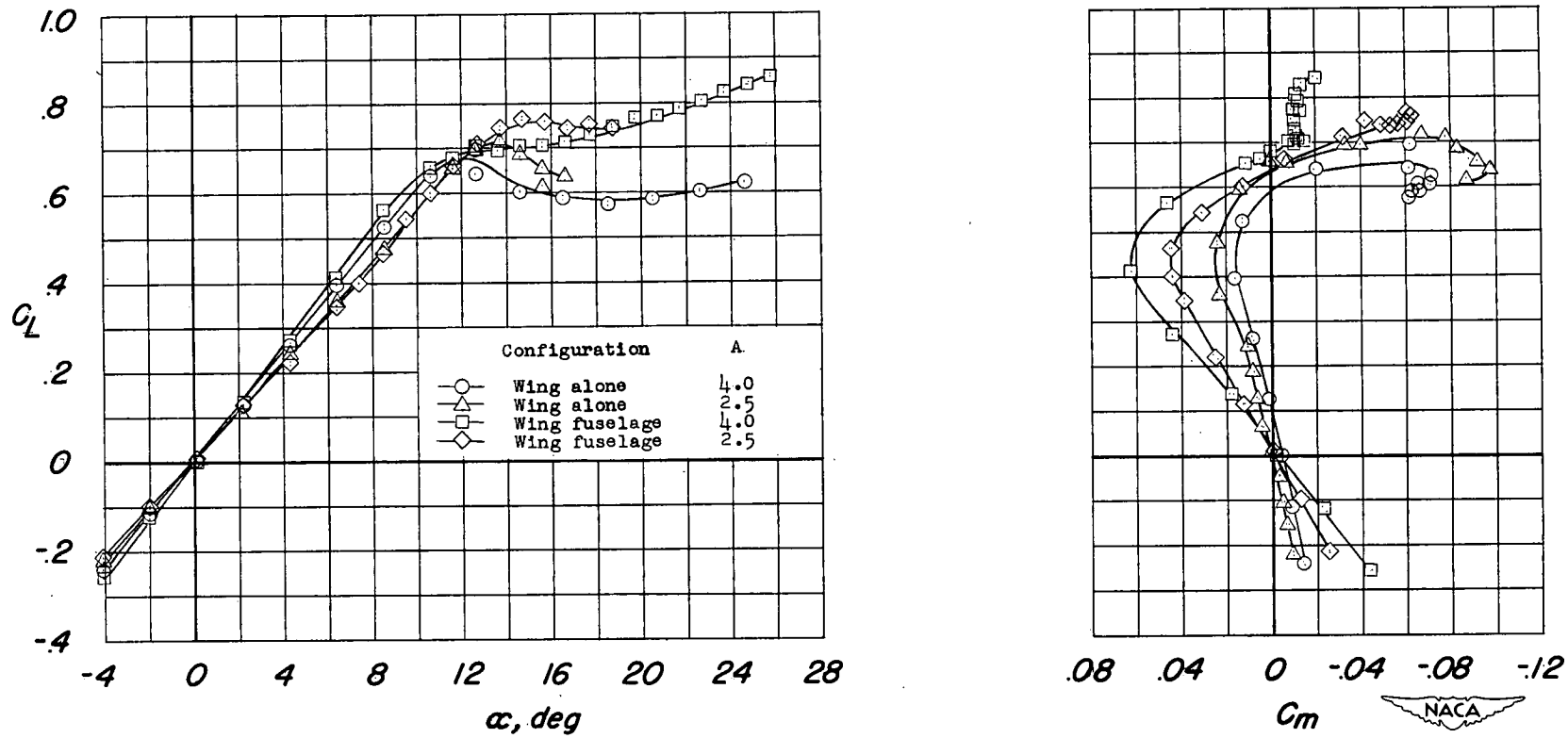

(a) Variation of lift coefficient with angle of attack and pitching-moment coefficient.

Figure 3.- Effect of fuselage on lift, drag, and pitching-moment characteristics of plain wing having aspect ratios of 4.0 and 2.5.

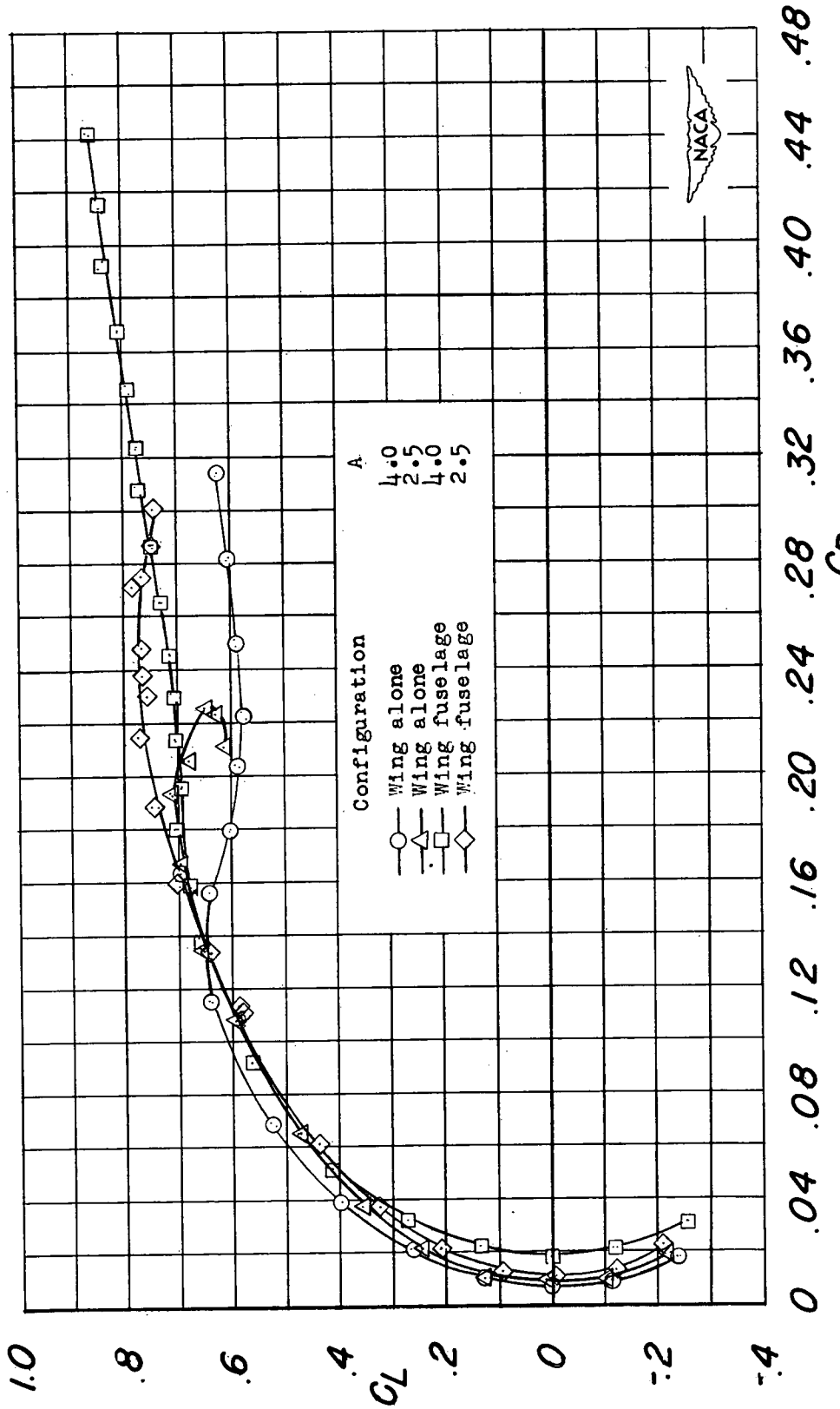

(b) Variation of lift coefficient with drag coefficient.

Figure 3.- Concluded.

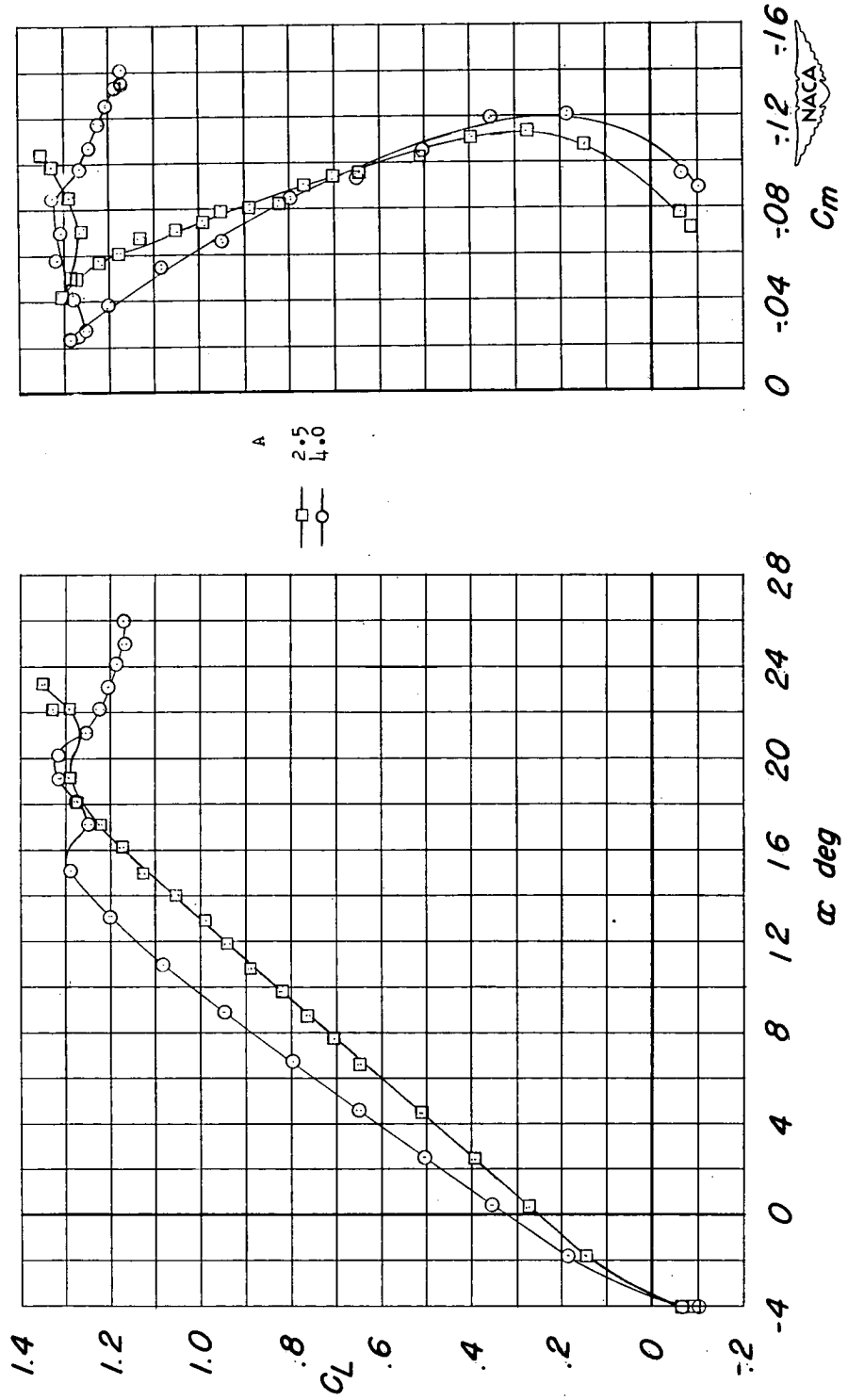

(a) Variation of lift coefficient with angle of attack and pitching-moment coefficient.

Figure 4.- Comparisons of lift, drag, and pitching-moment characteristics of the aspect-ratio-4.0 wing-fuselage combination with that of the aspect-ratio-2.5 wing-fuselage combination. Leading- and trailing-edge flaps are deflected.

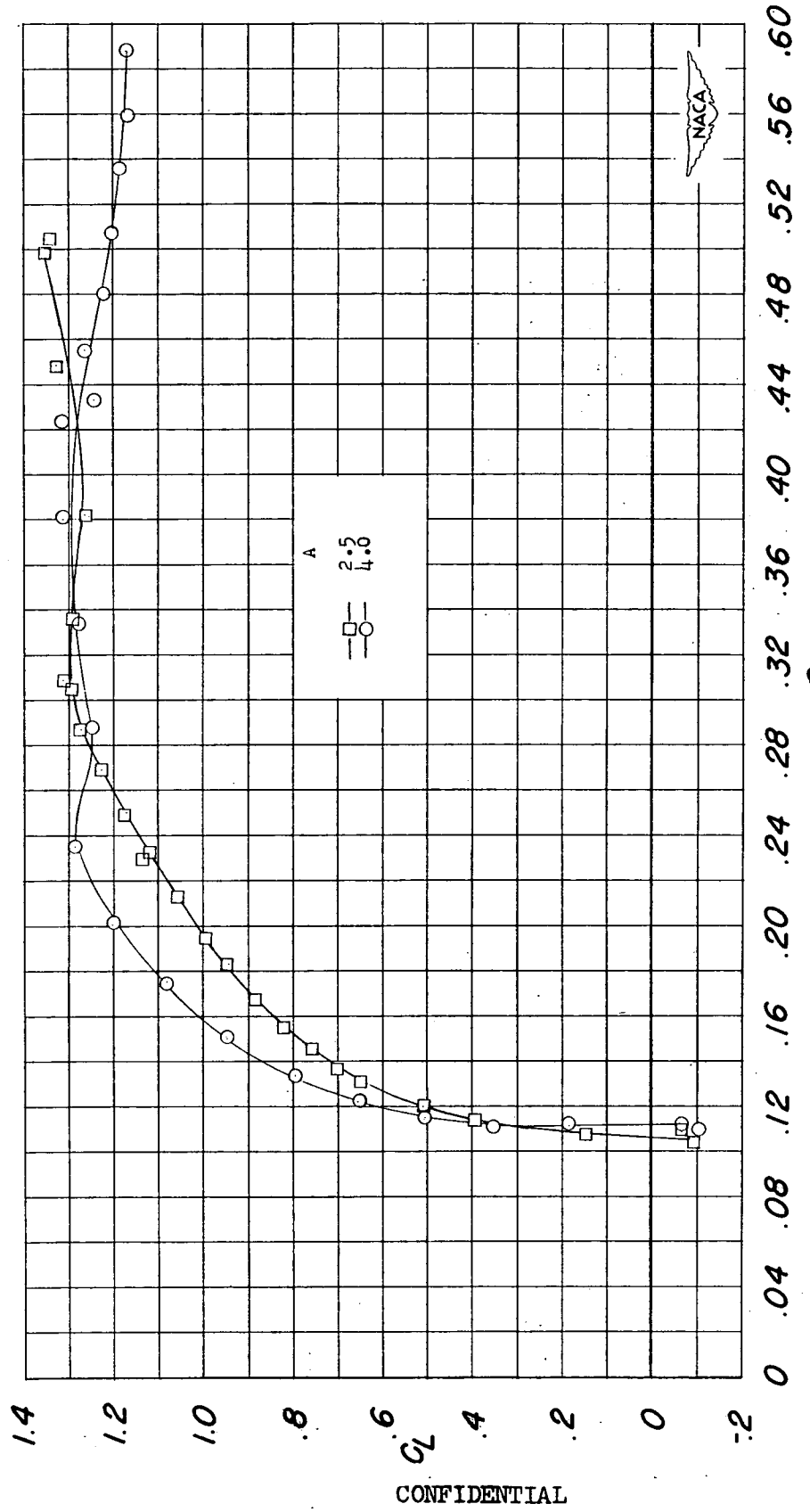

(b) Variation of lift coefficient with drag coefficient.

Figure 4.- Concluded.

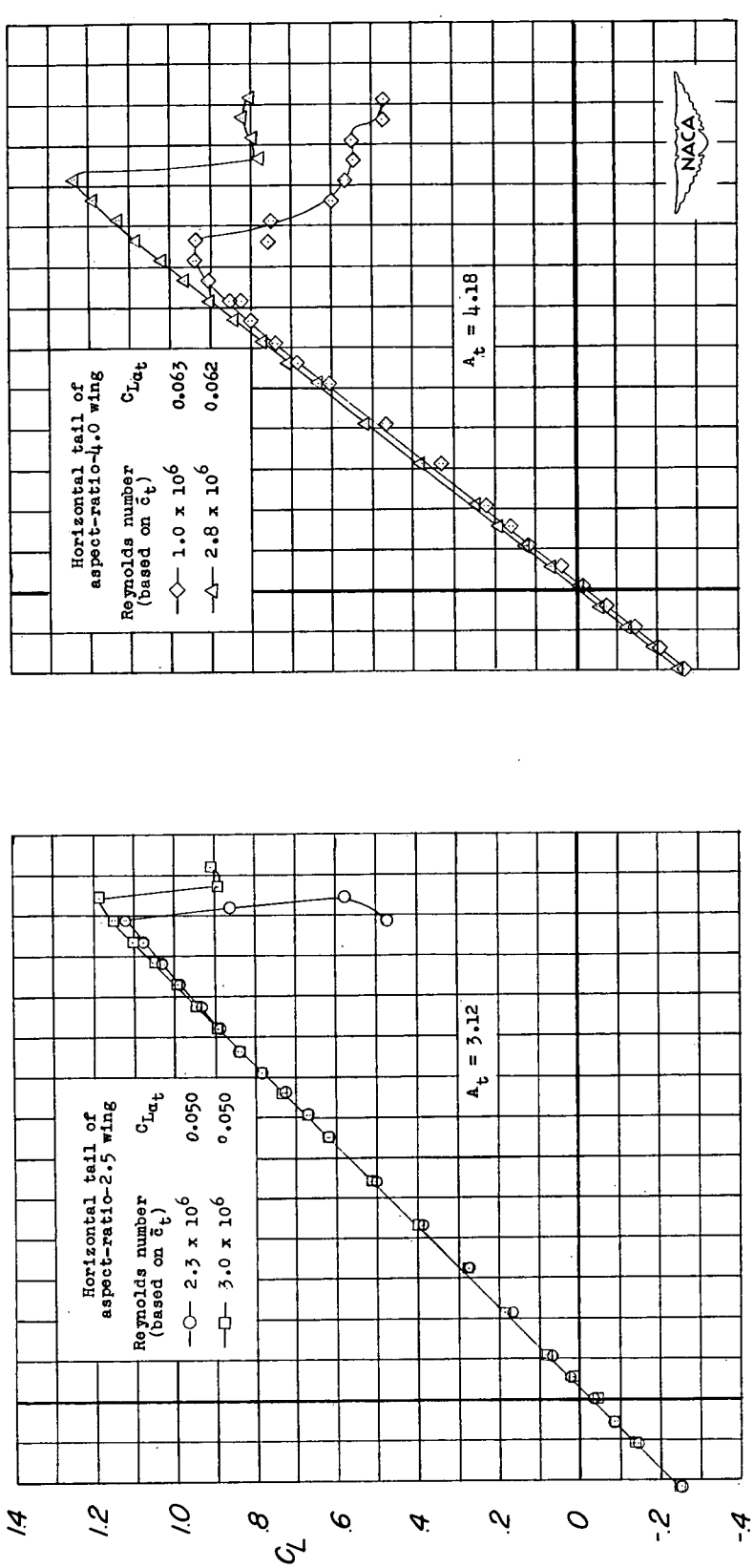

Figure 5.- Variation of lift coefficient with angle of attack of the two horizontal tails.

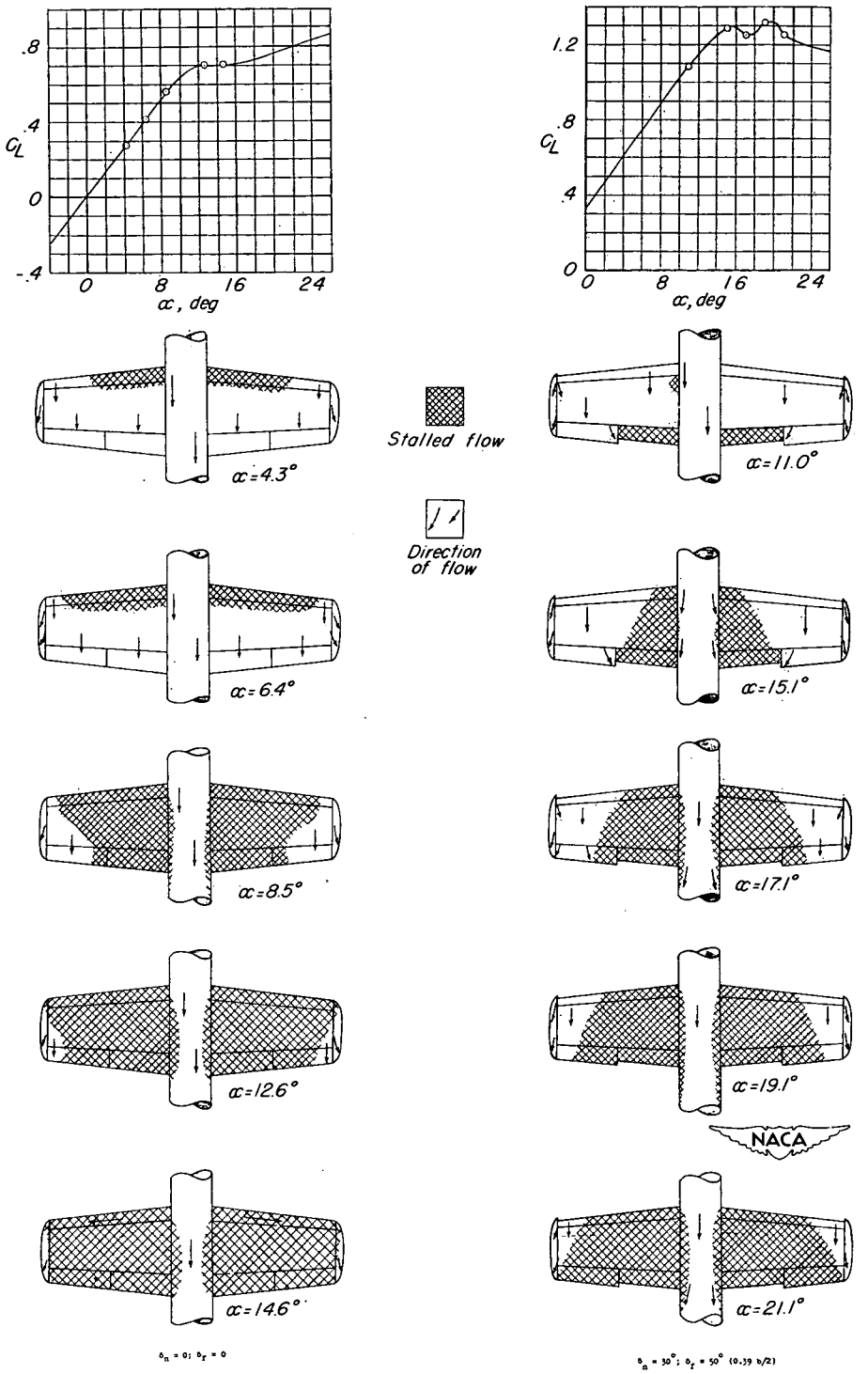

(a) Aspect ratio, 4.0.

Figure 6.- Stall patterns of aspect-ratio-4.0 and aspect-ratio-2.5 wings with and without leading- and trailing-edge flaps deflected.

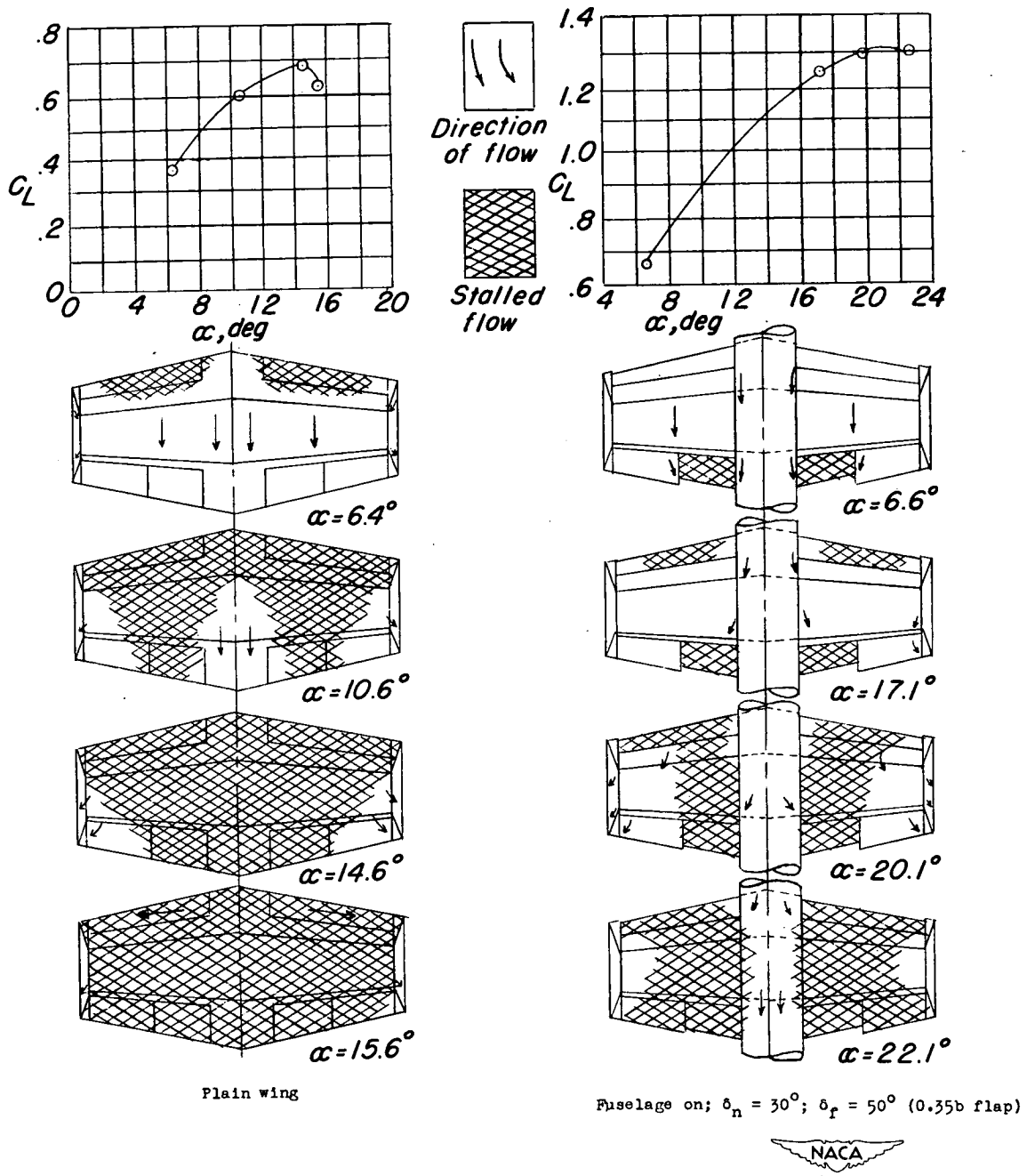

(b) Aspect ratio, 2.5.

Figure 6.- Concluded.

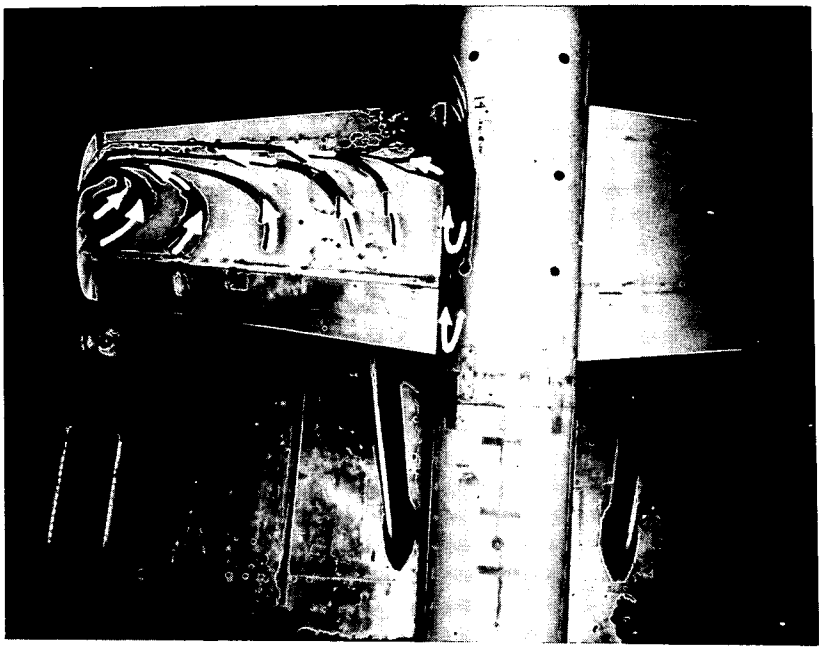

L-77584.1

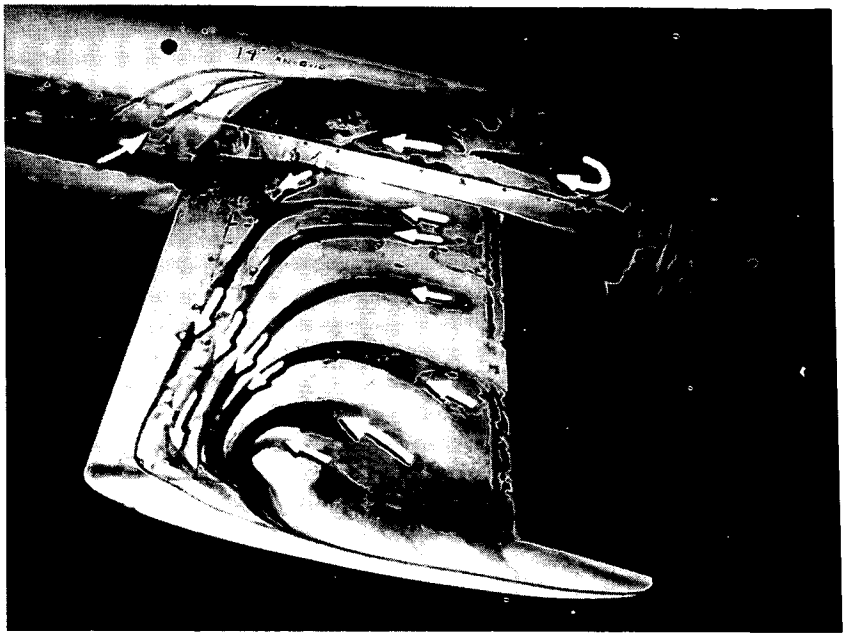

L-77586.1

(a) Plain-wing-fuselage configuration. $\alpha = 14.6^{\circ}$.

Figure 7.- Example of air flow over wing-fuselage combination of aspect-ratio-4.0 wing at stalled conditions.

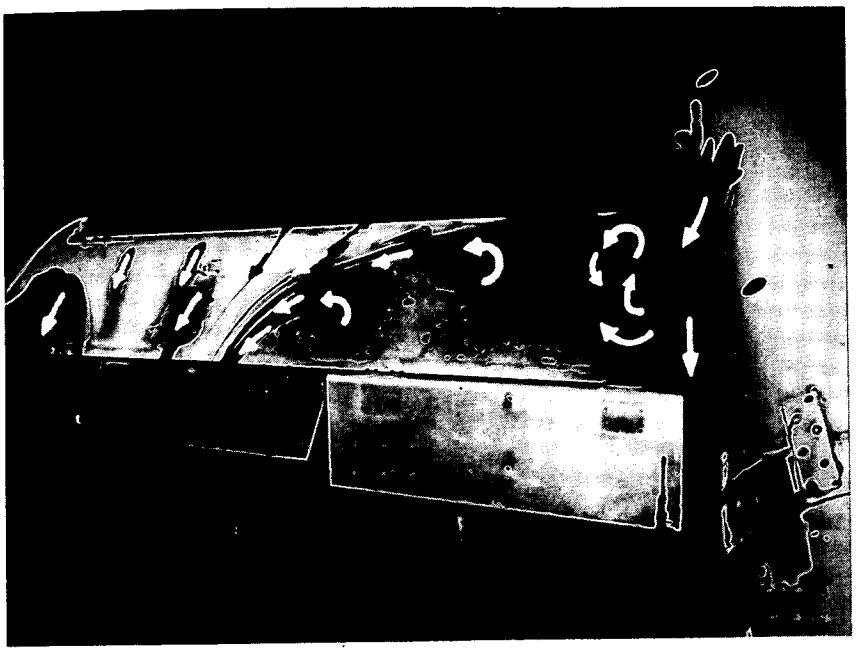

L-77582.1

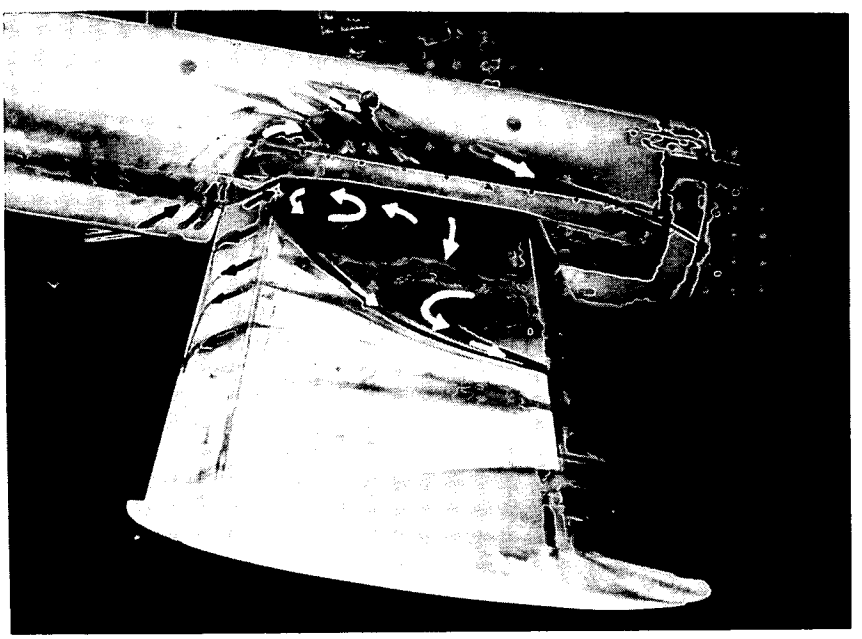

L-77583.1

(b) The 0.79b/2 leading-edge flap and 0.39b/2 trailing-edge flap deflected on wing-fuselage configuration. $\alpha = 18.1^{\circ}$.

Figure 7.- Concluded.

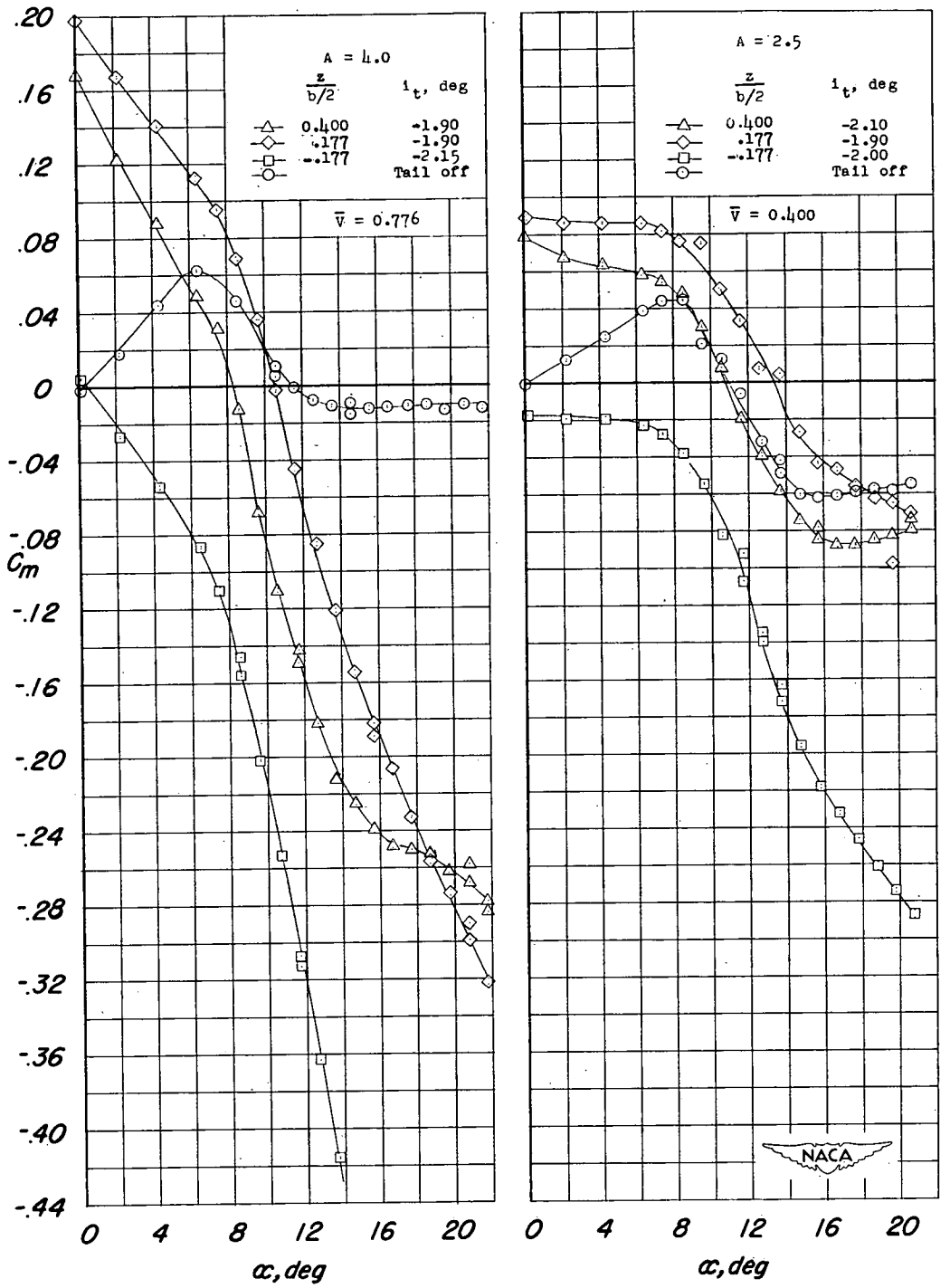

(a) Variation of pitching-moment coefficient with angle of attack.

Figure 8.- Comparisons of C_m, ϵ_e, and $(q_t/q)_e$ at various tail heights for the aspect-ratio-4.0 wing and the aspect-ratio-2.5 wing. Plain wing; fuselage on.

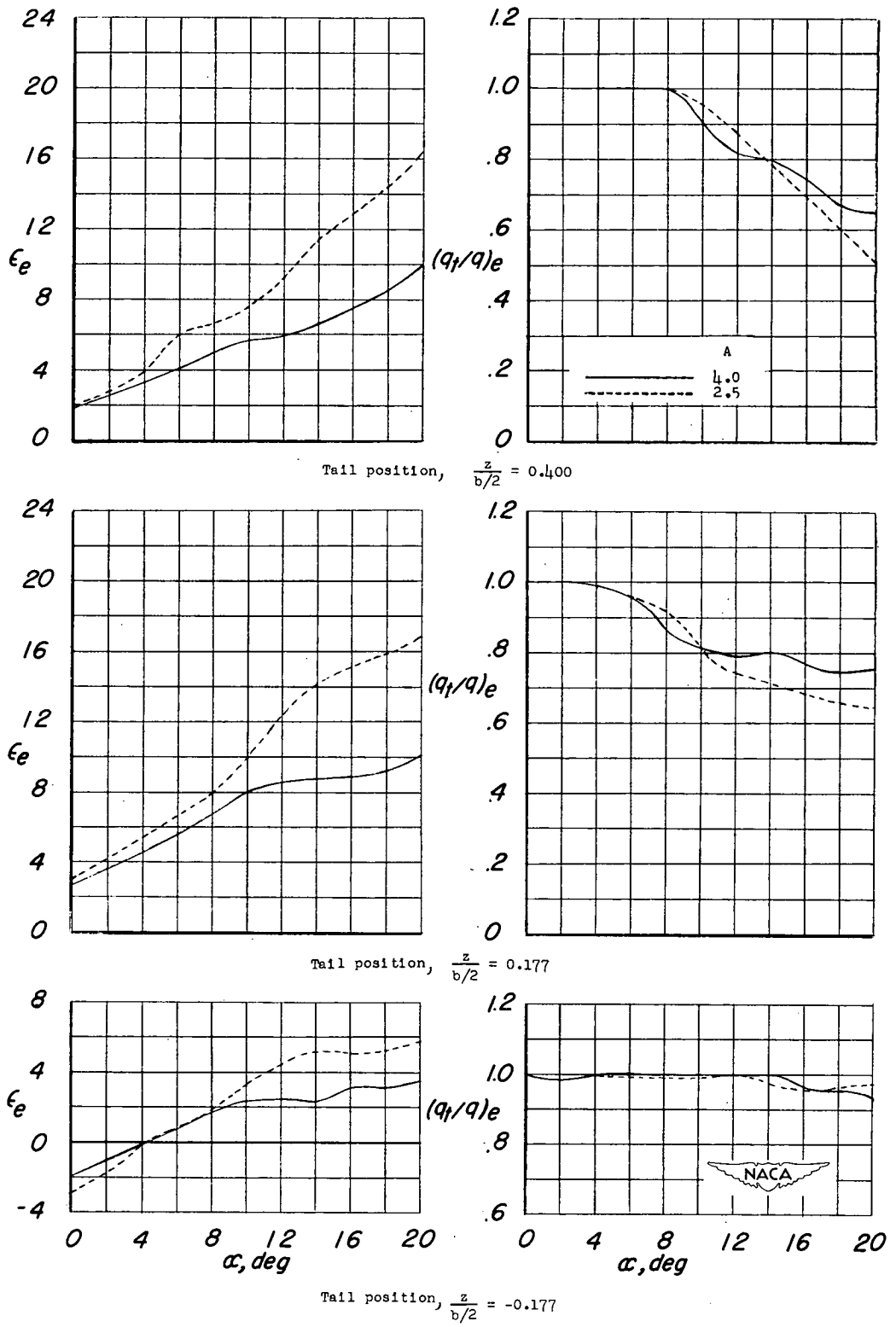

(b) Variation of downwash and dynamic-pressure ratio with angle of attack.

Figure 8.- Concluded.

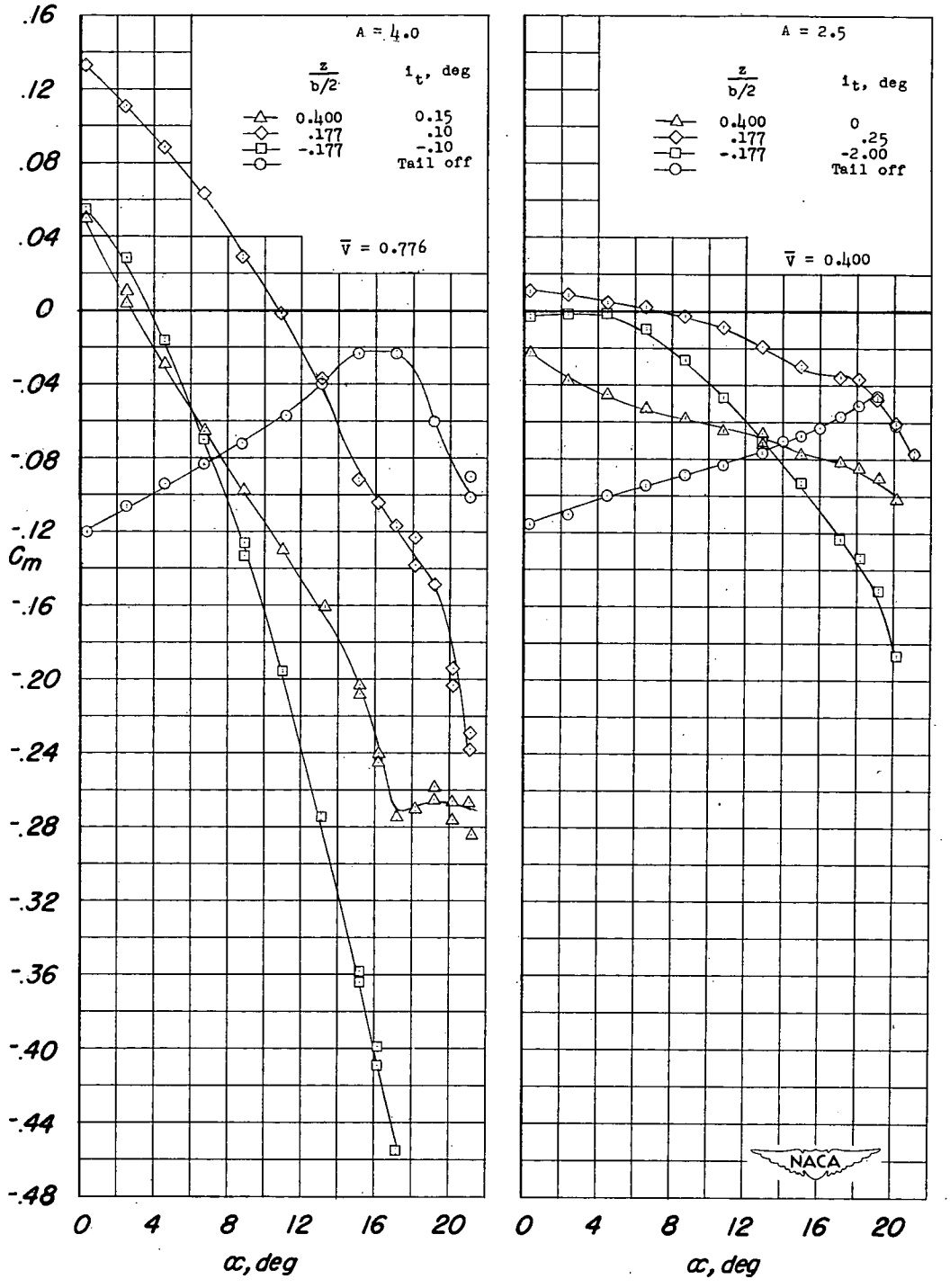

(a) Variation of pitching-moment coefficient with angle of attack.

Figure 9.- Comparisons of C_m, ϵ_e, and $(q_t/q)_e$ at various tail heights for the aspect-ratio-4.0 wing and the aspect-ratio-2.5 wing. Leading- and trailing-edge flaps deflected, fuselage on.

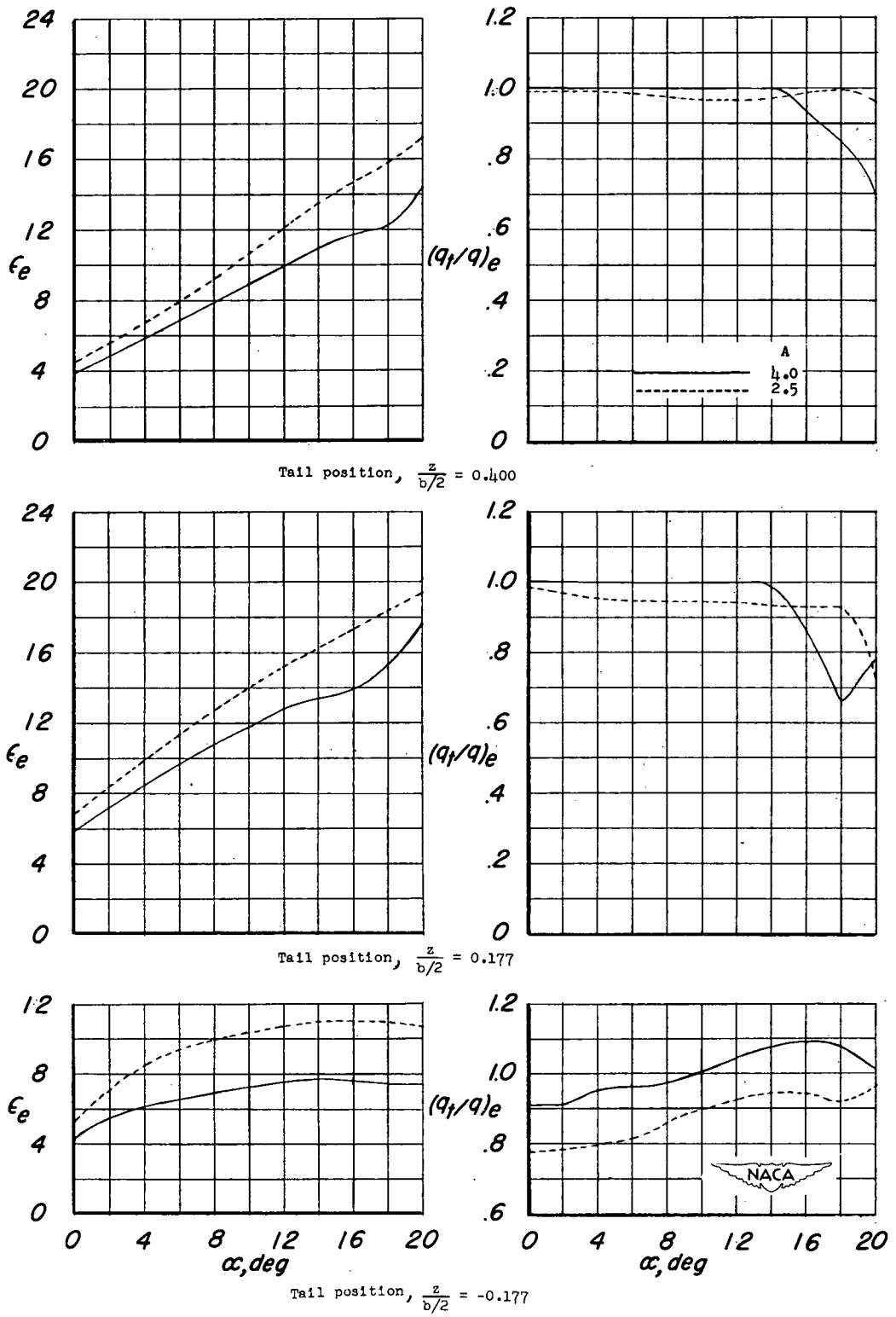

(b) Variation of downwash and dynamic-pressure ratio with angle of attack.

Figure 9.- Concluded.

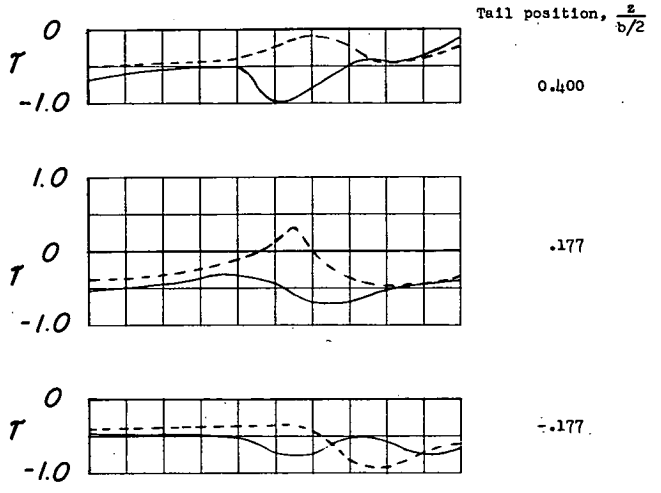

(a) Flaps undeflected.

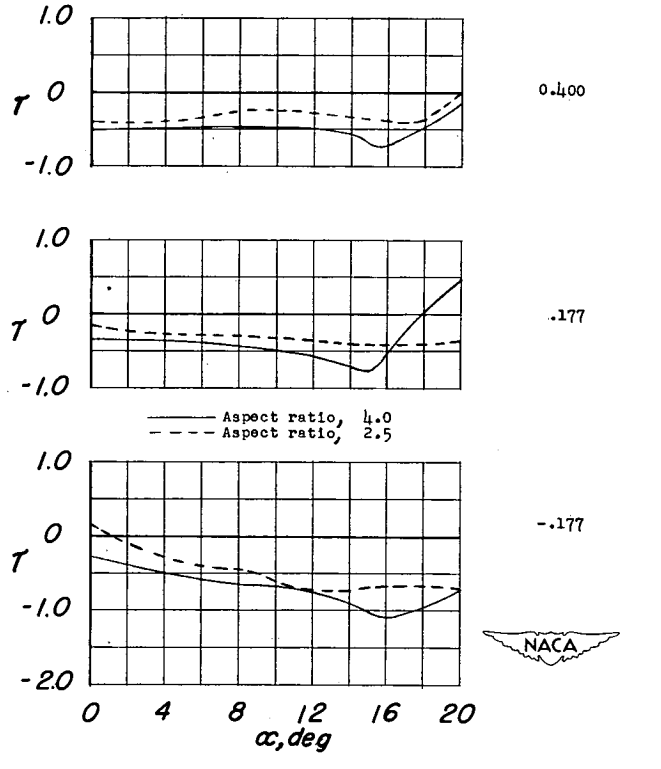

(b) Leading- and trailing-edge flaps deflected.

Figure 10.- Comparison of tail effectiveness parameter at various vertical-tail positions for the aspect-ratio-2.5 wing and aspect-ratio-4.0 wing.

NACA-Langley - 10-26-53 - 325